



Electron transmission through band structure in organized organic thin films

A. Haran^a, A. Kadyshevitch^a, H. Cohen^b, R. Naaman^{a,*}, D. Evans^{c,d},
T. Seideman^{c,e}, A. Nitzan^c

^a Department of Chemical Physics, Weizmann Institute of Science, 76100 Rehovot, Israel

^b Chemical Services, Weizmann Institute of Science, 76100 Rehovot, Israel

^c School of Chemistry, Tel-Aviv University, 69978 Tel Aviv, Israel

^d Department of Chemistry, University of New Mexico, Albuquerque, NM 87131, USA

^e Stacie Institute, National Research Council, Ottawa, Ont. K1A 0R6, Canada

Received 4 December 1996

Abstract

Direct evidence for the electronic band structure of thin organized organic layers is presented. The experimental results indicate that the electron–organic film system has to be described in quantum mechanical terms and that classical concepts fail. Quantum mechanical simulations on a generic system are also presented. They indicate that this type of simulation provides insight into the system studied experimentally.

1. Introduction

Electron transmission through organic thin films condensed on metal substrates has been investigated mainly by low-energy electron-transmission (LEET) spectroscopy (for a review, see Refs. [1,2]). It was established that for an ordered rare gas and other simple molecular layers the transmission [3,4], as well as the reflection [5,6] are strongly correlated with the band structure of the corresponding rare gas crystal. A similar behavior is expected for films of saturated hydrocarbon chains of various lengths [7]. The polymer thin films used in past studies were not ordered and it was therefore difficult to establish the effect of their organization on their electronic proper-

ties. In previous studies [8,9] two of us have demonstrated that such films are transparent to electrons of energy higher than 0.8 eV (above the vacuum energy), and Sanche has commented that this onset of unity transmittance is associated with the position at $V_0 = 0.8$ eV of the conduction band edge in hydrocarbon crystals [10]. Here we present further evidence for the effect of electronic band structure on the conductive properties of organized organic thin films (OOTFs).

Organized organic thin films have the advantage of being well defined in terms of orientation and packing. Due to their nature, it is possible to modify the thickness of the film in a controlled manner, layer after layer. The electron transport properties of OOTF have been studied extensively in the past (see Ref. [11] and references cited therein and Ref. [12]).

* Corresponding author.

In those studies, the current versus voltage applied on electrodes in contact with the OOTF was measured, without the ability to monitor the electron energy distribution. The possibility of pinholes in the organic film, which affect the measured resistivity, cast the quantitative analysis in uncertainty.

As noted above, we have found that electrons with energy larger than 0.8 eV can pass efficiently through OOTFs [8,9]. Here we present new experimental results as well as quantum simulations which give further support to the idea that this high transparency is associated with the layer band structure.

2. Experimental

2.1. Film preparation and characterization

The OOTFs were prepared by the Langmuir–Blodgett (LB) method [13,14] and transferred to a glass microscope slide coated with a 150 nm thick silver film prepared by vacuum evaporation. The film was treated with an ultraviolet ozone cleaner that removed organic contamination and formed an oxide layer that is stable when exposed to air/water. The photoelectron emission characteristics of the film and its morphology¹ are not affected by the ozone treatment. Silver was chosen as the substrate in the present studies because of its relatively low work function and chemical stability.

In the present study, the OOTFs consist of cadmium arachidate (CdAr), $(\text{CH}_3(\text{CH}_2)_{18}\text{COO}^-)_2\text{Cd}^2$ mono- and multilayers. The organic films were deposited using a Nima 611, GB trough. Arachidic acid was dissolved in chloroform (0.5 mg/ml) and was spread on an aqueous solution of 0.001 M CdCl_2 . The pH of the solution was adjusted to 8.5 by adding a small amount of ammonia. At this pH the CdAr films were transferred. The depositions were performed at a temperature of 22°C, a surface pressure of 27–28 mN/m and a lift speed of 1 cm/min. The quality of each film was determined by monitoring the area of the monolayer transferred onto the slide

from the water–air interface. For some of these films wettability measurements were performed. For successfully deposited films, the contact angle with water was 111–113°. The grazing angle Fourier transform infrared (FTIR) spectrum was measured for some of the films and the intensities of the C–H stretching bands (CH_3 asymmetric, CH_2 asymmetric, CH_2 symmetric at 2958, 2917, 2849 cm^{-1} respectively) were monitored. The absorption of the CH_2 asymmetric stretching band was compared for 1, 3 and 5 layers of CdAr, and a linear dependence of the absorption on the number of layers was observed.

2.2. Photoelectron energy distribution measurements

Two experimental systems were used to obtain the transmission function of photoelectrons through the OOTFs. In the first, a commercial UPS system was utilized (Kratos Analytical, AXIS-HS). The UV source was a helium lamp emitting mainly at the He(I) line (21.21 eV), due to the He pressure conditions — $(0.6\text{--}1.0) \times 10^{-7}$ mbar. In order to minimize damage to the organic film, the current through the lamp was reduced to the minimum required to obtain stable UV radiation (30mA). We examined the effect of OOTF on the secondary electron emission (SEE) peak of the silver substrate. Each set of a measurements comprised of measurement of two samples: a CdAr coated silver film and a bare silver film as a reference.

To account reliably for the peak shape of the slow (secondary) electrons, special experimental conditions were chosen. The magnetic lens was kept off, while each set of measurements proceeded by degaussing the residual magnetic fields in the UHV chamber. The sample was biased at -40 V to enhance the transmission of the analyzer, while the slit aperture, responsible for the angular acceptance as well as the aperture controlling the probed area were kept at a minimal opening (below 1°) to ensure minimization of the peak distortion by non-normal take-off angle electrons. With a bias voltage of -40 V, the secondary electron peak had a well defined shape, such that the zero of the electron energy scale could easily be defined within 0.1 eV accuracy.

¹ Atomic force microscopy studies were performed on the silver films before and after the ozone treatment [15].

The signal from silver coated with OOTF was found to be stable only for relatively short times. This problem originates from the e-beam induced damage to the OOTF. The results presented below were obtained from fresh samples whose exposure to the electron beam did not exceed three minutes.

In the second scheme, a similar experimental system as discussed in Refs. [8,9] was used. Slides coated with OOTF were attached to a temperature controlled holder and inserted into a UHV chamber pumped to below 10^{-8} mbar by adsorption and ion pumps. The 223 nm (5.56 eV) light with a pulse (10 ns long) energy of 0.1 μ J was obtained by mixing the output of a frequency doubled Nd:Yag pumped dye laser with a 1064 nm light from the Nd:Yag laser. The laser beam is introduced into the chamber and after reflecting from the sample it exits through quartz windows. The photoelectron kinetic energy distribution was measured via the retarding field method [16]. A grid made of nickel was placed 3 mm in front of and parallel to the silver/OOTF coated slide. The grid could be biased with a negative or positive voltage relative to the silver surface which was kept at ground potential. The close proximity of the grid and the silver surface ensures a high collection efficiency and non-perturbed collection of low-energy electrons. This kind of plane-parallel detector collects electrons according to the part of their kinetic energy corresponding to the velocity component perpendicular to the surface, E_{\perp} . If a negative potential $-V$ is applied to the grid, electrons with $E_{\perp} < eV$ cannot pass the mesh and therefore do not reach the detector.

A newly developed microsphere plate (MSP made by El-Mul, Israel) was placed 5 mm behind the grid and biased 200 V relative to it. The MSP serves as an electron multiplier, in the same way as does a regular microchannel plate. An anode placed behind the MSP collected the amplified electron signal, which was processed by a gated integrator (Stanford Research Systems). The laser pulse intensity was kept low so that nonlinear effects were eliminated.

The signal measured in this way is an integral of the emitted current over the emitted electron energy up to the energy corresponding to the voltage applied on the grid. Hence, by differentiating the signal with respect to grid voltage the emitted electron energy distribution is obtained.

3. Results and discussion

When the SEE peak was monitored for surfaces covered with OOTF, it was found to be narrower than the peak for the bare substrate. The results are presented in Fig. 1 as the transmission function through one (solid line) and 3 (dashed line) layers of CdAr. The transmission curve was calculated by dividing the electron signal at each electron energy, obtained from a silver film coated with the OOTF, by the electron signal of the bare silver film.

The low-energy part (< 1 eV) of the obtained curve is consistent with our previous results [8,9], whereas at higher energies new information is obtained. One observes a decrease in the transmission probability for electrons with energy above ca. 1.0 eV. This decrease is more abrupt, in terms of energies, when the film is composed of more layers.

The structure in the energy dependence of the transmission probability of electrons through a molecular layer can result from several origins. When the layers are thin enough, there are interference features associated with the width of the layer. Such features are observed even for a structureless barrier (Fig. 2a). For a barrier with discrete molecular struc-

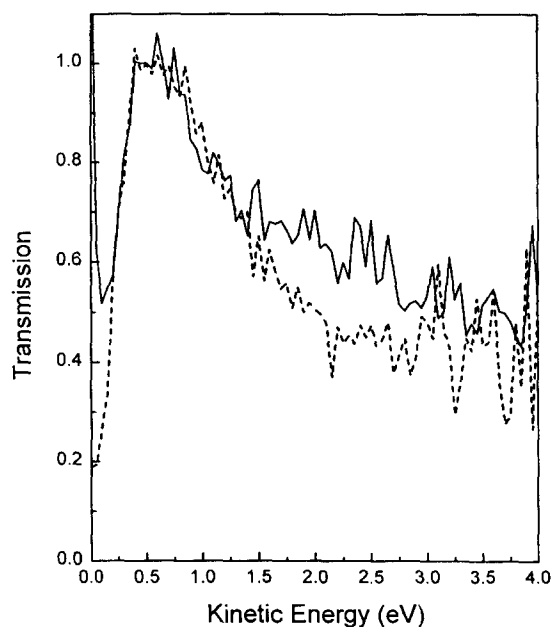


Fig. 1. The transmission probability of photoelectrons through one (solid line) and 3 (dashed line) layers of CdAr.

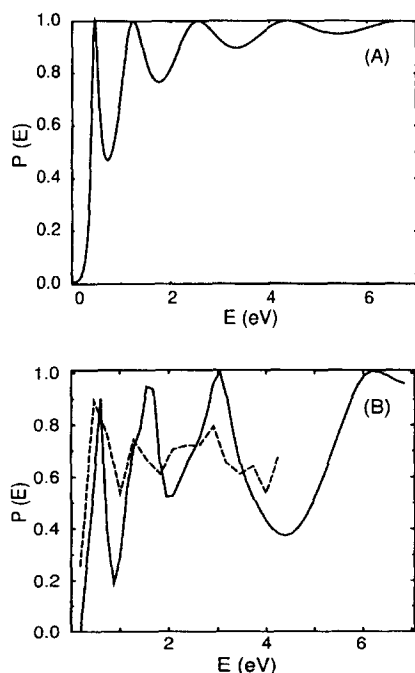


Fig. 2. (a) Transmission probability through a 1-d rectangular barrier characterized by height 3 eV and width 12 Å, as a function of incident electron energy measured relative to the barrier top. (b) Full line: electron transmission through a slab made of 4 Ar layers, cut out of an FCC Ar crystal in the (100) direction. Dashed line: same results obtained for a disordered Ar slab prepared as described in the text.

ture, the energy dependence of the transmission probability will also reflect the band structure of the underlying layer. Finally, below the conduction band edge, structure may originate from impurity/defect states in the gap [17]. The full line in Fig. 2b shows the transmission probability (summed over all final directions) vs. energy for an electron incident in the perpendicular direction on a slab of Ar atoms. This slab of 4 atomic layers thick was cut from an FCC lattice at a density corresponding to Ar at 4 K (1.77 g/cm³) in the (100) direction. The pseudopotential of Space et al. [18] was used for the electron–argon interaction, and the imaginary boundary conditions Green’s function method of Seideman and Miller [19,20] was used to evaluate the electron transmission probability (for details of this calculation see Ref. [21]). In addition to the interference features similar to those seen in Fig. 2a, a prominent dip in the transmission probability above 4 eV corresponds

to a band gap which is also observed experimentally. We note that the corresponding calculated gap in the density of states of bulk Ar is at 5 eV [22]; however, it seems that this gap shifts to lower energies thin layers [6]. The dashed line in Fig. 2b shows similar transmission results for a disordered Ar layer. This layer was prepared from the ordered one by annealing it at 400 K next to an adsorbing wall, using classical MD with Lennard-Jones potentials for the Ar–Ar interaction ($\epsilon = 120$ K and $\sigma = 6.4$ au) and for the Ar–wall interaction ($\epsilon = 115$ K and $\sigma = 6.4$ au)². The translational order parameter [23] of the resulting argon configurations was in the range 0.08–0.2. The dashed line in Fig. 2b represents an average over 4 configurations of the disordered slab obtained in this way. It is seen that the energy dependence of the transmission through the disordered layer is considerably less structured. In particular, the dip associated with the band gap has largely disappeared. It is likely that smoother shapes will be obtained with more configurational averaging.

For the CdAr system, even a monolayer is considerably thicker than the simulated system, so the energy dependence of the transmission through such layers will be dominated by the electronic band structure and/or impurity and defect states in these layers. X-ray studies indicate that, at room temperature, three layers of CdAr or more show clear crystalline diffraction, while a single layer is less ordered [24]. Hence it is expected that the band structure in the three layer system will be better defined, as indeed indicated by the sharper transmission band for an electron transmitted through three layers, compared to those transmitted through a single layer (Fig. 1).

The importance of film order to electron transmission is also demonstrated in Fig. 3a which presents the current density as a function of electron energy, for photoelectrons transmitted through 13 layers of CdAr before (squares) and after (triangles) they were heated to 378 K. The results were obtained by the home-built system using the retarded field method for the electron energy analysis. The results indicate

² During this annealing a featureless reflecting wall was placed 22 au away from the adsorbing wall, to prevent desorbing Ar atoms from escaping the simulated system.

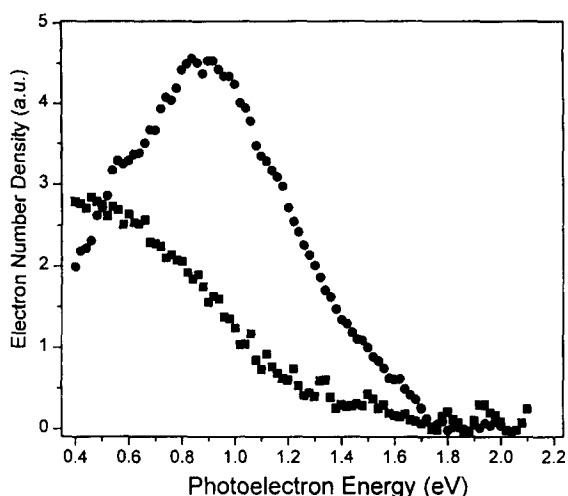


Fig. 3. The current density as measured by the retarding field method for photoelectrons transmitted through 13 organized (squares) and unorganized (triangles) layers of CdAr.

that while before heating electrons with energies above ca. 1 eV are transmitted through the band almost ballistically, after heating there is an efficient scattering process that suppresses the transmission peak similarly to what is observed in the dashed line of Fig. 2b.

At room temperature the structure of the CdAr film is crystal-like with orthorhombic symmetry. This structure is destroyed upon heating the films to 378 K and the amphiphilic chains are no longer ordered [24]. The change in structure is evident in the grazing angle IR spectra presented in Fig. 4. The increase in the intensities of the CH_2 absorption lines is an indication for the group being re-oriented, partially, so that the transition dipole moment associated with the vibrational excitation is not perfectly parallel to the surface, as in the ordered layers [25].

The results presented support the band structure model as an explanation for the efficient electron transmission through amphiphiles. This model may explain the high conductance through organic layers as measured with scanning tunneling microscopy [26] (STM). It also rationalizes the observation that electrons are better conducted through all-trans amphiphilic chains than through chains containing some gauche bonds: [27]. When the chains are in "all-trans" configuration, the layer is ordered and the electronic wavefunctions in the band are delocalized.

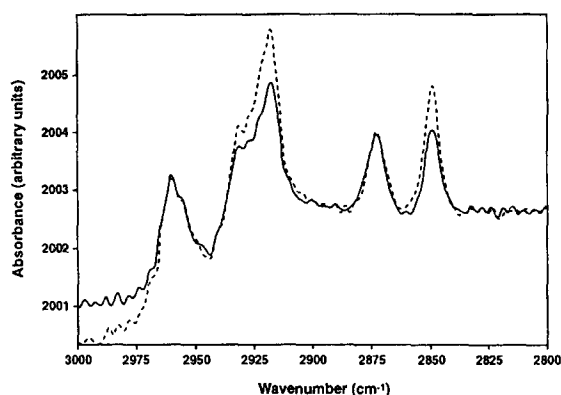


Fig. 4. The grazing angle IR spectra of 13 layers of organized CdAr (solid) and of the same films after they were heated to 378 K (dashed). The increase in the intensities of the CH_2 absorption peaks following the heating indicates the disorder in the film (see Ref. [25]).

The formation of gauche bonds amounts to introducing disorder which increases scattering and reflection and, when pronounced enough, localizes the electronic wavefunction and therefore reduces the conductivity through the organic chain.

Acknowledgements

This work was partially supported by the Ministry for Science and Art, Israel. RN thanks the partial support from the Israel Science Foundation and from the MINERVA Foundation.

References

- [1] L. Sanche, in: C. Ferradini, J.-P. Jay-Gerin (Eds.), *Excess Electrons in Dielectric Media*, CRC Press, Boca Raton, FL, 1991, Ch. 1, p. 1.
- [2] L. Sanche, *Scanning Microsc.* 9 (1995) 619.
- [3] G. Bader, G. Perluzzo, L.G. Caron, L. Sanche, *Phys. Rev. B* 30 (1984) 78.
- [4] G. Perluzzo, G. Bader, L.G. Caron, L. Sanche, *Phys. Rev. Lett.* 55 (1985) 545.
- [5] M. Michaud, L. Sanche, C. Gaubert, R. Baudoing, *Surf. Sci.* 205 (1988) 447.
- [6] T. Goulet, J.-M. Jung, M. Michaud, J.-P. Jay-Gerin, L. Sanche, *Phys. Rev. B* 50 (1994) 5101.
- [7] L.G. Caron, G. Perluzzo, G. Bader, L. Sanche, *Phys. Rev. B* 33 (1986) 3027.

- [8] A. Kadyshevitch, R. Naaman, *Phys. Rev. Lett.* 74 (1995) 3443.
- [9] A. Kadyshevitch, R. Naaman, *Thin Solid Films*, in press.
- [10] L. Sanche, *Phys. Rev. Lett.* 75 (1995) 2904.
- [11] P.S. Vincett, G.G. Roberts, *Thin Solid Films* 68 (1980) 135.
- [12] E.E. Polymeropoulos, J. Sagiv, *J. Chem. Phys.* 69 (1978) 1836.
- [13] K.B. Blodgett, *J. Am. Chem. Soc.* 57 (1935) 1007.
- [14] K.B. Blodgett, *Langmuir*, *Phys. Rev.* 51 (1937) 964.
- [15] K.S. Birdi, to be published.
- [16] L.A. DuBridge, *Phys. Rev.* 43 (1933) 727.
- [17] L.G. Caron, G. Perluzzo, G. Bader, L. Sanche, *Phys. Rev. B* 33 (1986) 3027.
- [18] B. Space, D.F. Coker, Z.H. Liu, B.J. Berne, G. Martyna, *J. Chem. Phys.* 97 (1992) 2002.
- [19] T. Seideman, W.H. Miller, *J. Chem. Phys.* 96 (1992) 4412.
- [20] T. Seideman, W.H. Miller, *J. Chem. Phys.* 97 (1992) 2499.
- [21] D. Evans, T. Seideman, H. Tal Ezer, A. Nitzan, to be published.
- [22] N.C. Bacalis, D.A. Papaconstantopoulos, W.E. Pickett, *Phys. Rev. B* 38 (1988) 6218.
- [23] M.P. Allen, D.J. Tildesley, *Computer Simulation of Liquids*, Oxford Press, 1989.
- [24] P. Tippmann-Krayer, R.M. Kenn, H. Mohwald, *Thin Solid Films* 210/211 (1992) 577.
- [25] S.R. Cohen, R. Naaman, J. Sagiv, *J. Phys. Chem.* 90 (1986) 3054.
- [26] J.A. DeRose, R.M. Leblance, *Surf. Sci. Rep.* 22 (1995) 75.
- [27] A. Haran, D.H. Waldeck, R. Naaman, E. Moons, D. Cahen, *Science* 263 (1994) 948.